INSTITUTO NACIONAL DE TECNICA AEROESPACIAL
«ESTEBAN TERRADAS»

FINAL REPORT

"ZERO-G GAUGING SYSTEMS"

CONTRACT No 17/8/4

Authors:

J. R. Sanmartín
E. Fraga
A. Muñoz

June, 1972

MADRID
SPAIN

F I N A L R E P O R T

"ZERO-G GAUGING SYSTEMS"

CONTRACT No 17/8/4

Authors:

J.R. Sanmartin
E. Fraga
A. Muñoz

June, 1972

A B S T R A C T

Various systems for measuring propellant content in spacecrafts under weightlessness conditions are reviewed. The cavity resonator method is found to be the most suitable measurement technique. This method is analyzed in detail. A determination of errors intrinsec to the method is carried out.

- - - - - -

I N D E X

- - - - -

STUDY OF VARIOUS TECHNIQUES FOR MEASURING PROPELLANT CONTENT IN SPACECRAFTS IN WEIGHTLESSNESS CONDITIONS

- - - - -

I. *INTRODUCTION*

This is the final report of ELDO Contract No. 17/8/4 "Zero G Gauging Systems". It includes first the selection of a promising system suitable for gauging liquid propellants contained in the tanks of a spacecraft with a specific application to the tanks of the Shuttle vehicle (Orbiter); and second a study of the selected system.

Propellant gauging in the Shuttle vehicle presents some important difficulties and additional problems as compared with the case of a conventional aircraft. Among these, the principal is that the vehicle will be operating under zero-g or low-g conditions during some stages of its operation.

Under stationary conditions in zero-g or low-g field, the geometrical configuration of the propellant in a spacecraft tank is dictated by the surface tension forces. When the acceleration increases, the shape that the propellant will adopt, will be depending upon the relative importance of the surface tension forces. Viscosity forces may be neglected due to the fact that the gradients of velocity that will appear in an actual case will

be small.

The available experimental evidence shows that surface tension governed configurations break up if the Bond number,

$$\text{Bond} = \frac{\text{Acceleration Forces}}{\text{Surface Tension Forces}} = \rho \frac{L^2 a}{\sigma}$$

is greater than a number of the order of 1. (Table I).

This Bond number criterion shows that the greater is the tank the smaller is the acceleration that may disrupt a capillary governed configuration in it.

The Shuttle will be subjected to a great number of acceleration perturbations. Orientation maneuvres, separation and docking of vehicles, equipment and crew movement, atmospheric drag in low orbits, will produce a random distribution of the propellant in the tanks.

For this reason the principal constraint for the gaging system in this specific case is the lack of knowledge on the propellant configuration in the tank. Furthermore, the cryogenic nature of propellants and the hazardous environment surrounding the spacecraft has to be taken into account.

Another important requirement to be considered is to re-

duce the interference of the propellant gauging system with the rest of the Shuttle vehicle.

In order to fulfill this requirement the selected system should have:

a) Reasonable weight and size.

b) Low power consumption

c) Few tank modifications (holes, structures ...)

II. SELECTION OF A GAUGING SYSTEM

II.1 TECHNICAL SPECIFICATIONS

The details of the final configuration of the tanks of the Shuttle vehicle are not yet known. For this reason, the available data will be completed with some reasonable assumptions.

Data.-

a) Propellants : LOX and LH_2 (Table II).

b) Size and shape as given by ELDO (see fig.1).

c) Material of the tank wall: Aluminium Alloy (for this study supposed rigid).

d) Inner PVC or PU foam insulation.

e) Tank vented. Pressure range form 17 to 30 p.s.i.a.

f) No provisions for bladder or any positive expulsion method.

Assumptions

a) Number of measurements is not limited, but these measurements may be discrete.

b) Overall response time: less than 5 seconds.

c) Initial ullage volume: 2% of total tank capacity.

d) Range of working temperature for the elements of the system placed outside the tank: -50°C to +100°C.

e) Power supply voltage: 24 to 30 V D.C.

f) Accuracy: desirable ±2% of full scale.

g) The output of the system should be processed in the spacecraft.

II.2 *POSSIBLE SYSTEMS TO BE USED FOR GAUGING PROPELLANTS*

Several gauging systems have been proposed in the literature as possible systems to gage propellant tank content in zero-g conditions.

A list of these methods, including a brief explanation of their working principles, is shown below.

Propellant Flow Integration.- The gauging is performed by measuring the propellant consumption by different methods.

Capacitance Systems.- They are based upon the variation of electrical capacity between conductors placed inside the tank, as the propellant is being consumed.

Isotope Technique.- These systems measure the absorption by the propellant mass, of a nuclear radiation produced by a radiactive source.

Pressure Response to Volume Perturbations.- Volume perturbations are introduced in the tank and the propellant mass is

deduced from the measurement of the pressure response.

Tracer Gas.- This method is based upon the measurement of the partial density of a tracer gas, previously introduced in the ullage volume.

Cavity Resonator.- The fundamental frequency of resonance of the tank, considered as a resonant cavity, and being excited by RF. would be measured.

A short discussion of the application of all the above-mentioned systems to the Shuttle vehicle is included in the following section.

II.3 *SELECTION OF A SYSTEM*

Propellant Flow Integration.- These systems introduce cumulative errors due to the nature of the measuring method. In addition, flow rate changes originated by throttling of the rocket engines would make more difficult to carry out accurate measurements. Those difficulties might be overcome, but there exists the fundamental problem of propellant losses through leakages or venting which would not be detected.

Isotope Techniques.- This system requires a great number of emitters and a very complicated hardware, if the measurements

are to be independent of the propellant configuration inside the tank. The analysis of the measurement data resulting from this arrangement would be complex and the required hardware would be cumbersome. Only a single emitter and the corresponding detector would be necessary in the case of tanks of aspect ratio of 50 or more. In this type of tank the utilization of isotope techniques for gauging propellant would be of interest.

Pressure Response to Volume Perturbations.- These systems have been treated in the literature under the name of "Gas Law Systems". It would be possible to employ these techniques if the volume perturbations required to produce a measurable pressure response were to be reasonably small.

For the Shuttle case, according to ELDO data, for a tank volume of the order of 200 m^3, if a pressure variation of 0.05 kg/cm^2 is specified, the perturbation volume required will be of 0.1 m^3. This figure seems to be too high to be employed in an actual system.

In the case of propellant tanks for satellite propulsion (volume less than 0.1 m^3) this system seems to be attractive.

Tracer Gas.- The measurement is performed in this system under the assumption that the mass of a tracer gas in the ullage volume of the tank is constant.

Tracer gas solution in the propellant, tracer gas losses through the venting or propellant outlet or tracer gas leakages make this assumption to be very doubtful. This problem might be probably overcome if a recalibration is carried out before each measurement is performed. This would greatly increase the complexity of the system.

Capacity System.- There is some experience in capacity gauging of liquids. NASA awarded a contract in 1967 to study the feasibility of such method for use in spacecraft tanks. One of the principal conclusions of this work [1] has been that, in order to perform a measurement independent of the propellant shape it is required to establish an uniform electrical field inside the tank. The electrical field would be obtained by giving an appropriate distribution of potentials to a number of conductors placed in the inner surface of the tank walls. In some particular case (spheres, cylinders of high aspect ratio) a limited number of electrodes would be required in order to produce an electrical field sufficiently uniform. When the tanks have another geometrical configurations, the problem requires a further analysis.

The placement of electrodes in the inner surface of a tank, including the insulation between their edges, would pose some technological problems. If the number of electrodes is

not too large this problem appears to be feasible.

An important study which is required in order to establish the feasibility of a capacitive gaging system is the definition of the method which would be employed for measuring the electrical capacity existing among the electrodes when considering the propellant as a dielectric. It is thought that by using the existing technologies it is possible to devise such measuring system. However, the great capacity existing among the electrodes and the tank wall will complicate considerably the acquisition of an accurate measurement.

It has been concluded that although a capacitive gauging system would be in principle feasible, the need of placing electrodes in the inner wall of the tank would make fabrication complex and cumbersome. For this reason the capacitive gauging system has been considered as an alternative solution to be studied in case in which the most promising system,"Cavity Resonator System" as indicated below,would not be feasible.

Cavity Resonator Systems.- The idea of gauging propellant in a tank considering it as a resonant cavity for electromagnetic modes has been proposed in the past. The principal question on which the feasibility of the system essentially depends, is whether or not the frequency of resonance is influenced by the propellant configuration.

This is a difficult problem since its rigorous, theoretical treatment requires the analysis of the Maxwell equations with very complicated boundary conditions. In Part II of this report, this problem is studied and solved.

The electrical properties of the propellants LH_2 and LOX (see Table II) are adequate in order to use a gauging technique of this type. They may be considered as good dielectrics with extremely high electrical resistivity. On the other hand, the relative dielectric constants are small enough to reduce the influence of different configurations for the same amount of propellant in the output of the system and they are high enough to allow sustantive change of resonant frequency between empty and full tank. The existence of an inner heat shield will not produce additional difficulties for the application of this method due to the fact that generally the heat insulation materials are good dielectrics and the foam structure increases this property. For all those reasons the electromagnetic waves will be attenuated very slowly inside the tank, the Q of the cavity will remain in all conditions very high and the power required in order to mantain the oscillations in the cavity will be small.

A rough estimation of the order of the resonant frequency for the first mode has been done considering the largest LOX and LH_2 tanks when they are empty.

The first mode for the LH_2 tank gives a resonance frequency of:

$$fLH_2 = 250 \text{ Mc/s.}$$

and for the largest LOX tank

$$fLOX = 330 \text{ Mc/s.}$$

Production, coupling and detection of such frequencies to and from the cavity is well below the present state of the art of the electronics. In general the technical details of this method appear to be much less complicated than those of all other methods.

A detailed review of all abovementioned methods can be found elsewhere [2].

III. STUDY OF THE CAVITY RESONATOR METHOD

- - - - - -

As it is well known, the purpose of the cavity resonator method is to infer the propellant content in a tank from the shift in the frequency of one of the resonant modes of the cavity; unfortunately, this shift should also depend, in general, on the propellant configuration, and this can not be exactly predicted because of the weightlessness condition.

Previous theoretical and experimental studies |3| , |4| , |5| of the configuration dependency have, in our opinion, been unconvincing. This part of the report includes a theoretical analysis of this point; we find that, in general, the frequency shift does depend on the propellant configuration. Nevertheless, we also find that, under particular conditions of practical interest, this dependency can be made acceptable so that the measurements of the frequency shift will indeed determine the propellant content. In particular, we show that this is the case of the Shuttle vehicle tanks.

III.1 GENERAL FORMULA FOR THE FREQUENCY SHIFT

The microwave cavity perturbation method, a technique frequently used in plasma diagnostics, is based on the fact that the resonant frequency of a microwave cavity resonator is changed when a plasma is introduced inside the cavity. This problem,

which is mathematically identical to the present one, has been extensively analyzed in the literature. Below, we resume the main mathematical steps leading to a general expression for the frequency shift [6][7] .

Consider a cavity of arbitrary shape and conducting walls, which in a first case is empty, and in a second case is filled with a substance of dielectric constant ε (in general a function of space coordinates). Writing Maxwell's equations for these two cases, we have [8]

$$\nabla \wedge \vec{E}_i = -j\omega_i \mu_o \vec{H}_i \quad , \tag{1}$$

$$\nabla \wedge \vec{H}_i = j\omega_i \varepsilon_o \varepsilon_i \vec{E}_i \quad , \tag{2}$$

where $i = 1$ for the first case, $i = 2$ for the second one, and $\varepsilon_1 = 1$, $\varepsilon_2 = \varepsilon$. $\vec{E}_i$ and $\vec{H}_i$ are the fields inside the cavity, which are assumed to have a temporal dependency of the form $\exp(j\omega_i t)$. The boundary conditions are that, at the cavity walls, $\vec{E}_i$ must be normal, and $\vec{H}_i$ tangential, to the walls, that is

$$\vec{H}_{in} = 0 \quad , \quad \vec{E}_{it} = 0 \quad . \tag{3}$$

From Eqs. (2) ($i = 1, 2$) we immediately obtain

$$j\varepsilon_o \int_{V_c} \left[\omega_1 - \omega_2 \varepsilon\right] \vec{E}_1 \cdot \vec{E}_2 dV = \int_{V_c} \left[\vec{E}_2 \cdot \nabla \wedge \vec{H}_1 - \vec{E}_1 \cdot \nabla \wedge \vec{H}_2\right] dV =$$

$$= \int_{\Sigma_c} \left[\vec{H}_1 \wedge \vec{E}_2 - \vec{H}_2 \wedge \vec{E}_1\right] \cdot d\vec{\Sigma} + \int_{V_c} \left[H_1 \cdot \nabla \wedge \vec{E}_2 - \vec{H}_2 \cdot \nabla \wedge \vec{E}_1\right] dV \qquad (4)$$

where V_c and Σ_c are the volume and surface of the cavity respectively, and we have used Gauss' theorem to obtain the last equality. Because of the second boundary condition in Eq.(3) the surface integral vanishes.

Similarly, from Eqs.(1) $(i = 1,2)$ we get

$$j\mu_o(\omega_1 - \omega_2) \int_{V_c} \vec{H}_1 \cdot \vec{H}_2 dV = \int_{V_c} \left[\vec{H}_1 \cdot \nabla \wedge \vec{E}_2 - H_2 \cdot \nabla \wedge \vec{E}_1\right] dV \qquad (5)$$

and finally, from Eqs.(4) and (5), |6|

$$\frac{\omega_2 - \omega_1}{\omega_2} = - \frac{\varepsilon_o \int_{V_c} (\varepsilon - 1) \vec{E}_1 \cdot \vec{E}_2 dV}{\varepsilon_o \int_{V_c} \vec{E}_1 \cdot \vec{E}_2 dV - \mu_o \int_{V_c} \vec{H}_1 \cdot \vec{H}_2 dV} \,. \qquad (6)$$

Usually the microwave cavity plasma diagnostic tecnique is used under such conditions that $\varepsilon \approx 1$ so that $\omega_2 \approx \omega_1$ and Eq. (6) becomes |6|

$$\frac{\omega_2 - \omega_1}{\omega_1} \simeq - \frac{\varepsilon_o \int_{V_c} (\varepsilon-1) E_1^2 dV}{\varepsilon_o \int_{V_c} E_1^2 dV - \mu_o \int_{V_c} H_1^2 dV} = - \frac{\int_{V_c} (\varepsilon-1) E_1^2 dV}{2 \int_{V_c} E_1^2 dV} \quad (7)$$

where we used the equality

$$\varepsilon_o \int_{V_c} E_1^2 dV = - \mu_o \int_{V_c} H_1^2 dV \quad (8)$$

which can be easily obtained from Eqs.(1) and (2) (i = 1).

In the case of interest to us, we have $\varepsilon = \varepsilon_L$ (a constant) in the region occupied by the propellant liquid, and $\varepsilon = 1$ in the rest of the cavity, since the propellant vapor has a dielectric constant practically equal to unity. Thus, ε is then a discontinuous function; it is possible to show however that, since H_2 is still continuous, Eqs. (6) and (7) are valid even for ε discontinuous.

Equation (6) takes now the form

$$\frac{\omega_2 - \omega_1}{\omega_2} = - \frac{\varepsilon_o (\varepsilon_L - 1) \int_{V_c} \vec{E}_1 \cdot \vec{E}_2 \, dV}{\varepsilon_o \int_{V_c} \vec{E}_1 \cdot \vec{E}_2 dV - \mu_o \int_{V_c} \vec{H}_1 \cdot \vec{H}_2 dV} \quad (6a)$$

where V_L is the volume occupied by the liquid. For $\varepsilon_L \simeq 1$,

Eq. (6a) becomes

$$\frac{\omega_2 - \omega_1}{\omega_1} \simeq - \frac{\varepsilon_L - 1}{2} \frac{\int_{V_L} E_1^2 dV}{\int_{V_c} E_1^2 dV} \qquad (7a)$$

We have further found that Eqs.(6) and (6a) can be simplified by using the equality

$$\frac{\omega_1}{\omega_2} \varepsilon_o \int_{V_c} \vec{E}_1 \cdot \vec{E}_2 dV = -\mu_o \int_{V_c} \vec{H}_1 \cdot \vec{H}_2 dV \quad . \qquad (9)$$

To derive Eq.(9) we multiply Eq.(1) ($i = 2$) by $\vec{H}_1$ and integrate over V_c to obtain

$$-j\omega_2\mu_o \int_{V_c} \vec{H}_1 \cdot \vec{H}_2 dV = \int_{V_c} \vec{H}_1 \cdot \nabla \wedge \vec{E}_2 dV = \int_{\Sigma_c} (\vec{E}_2 \wedge \vec{H}_1) \cdot d\vec{\Sigma} +$$

$$+ \int_{V_c} \vec{E}_2 \cdot \nabla \wedge \vec{H}_1 dV = \int_{V_c} \vec{E}_2 \cdot \nabla \wedge \vec{H}_1 dV \qquad (10)$$

where Eq.(3) was used. Multiplying Eq.(2) ($i = 1$) by $\vec{E}_2$ and integrating over V_c we get

$$j\omega_1\varepsilon_o \int_{V_c} \vec{E}_2 \cdot \vec{E}_1 dV = \int_{V_c} \vec{E}_2 \cdot \nabla \wedge \vec{H}_1 dV \quad . \qquad (11)$$

From Eqs.(10) and (11), Eq.(9) follows immediately.

Equation (6a) then becomes

$$\frac{\omega_2 - \omega_1}{\omega_2}\left(1 + \frac{\omega_1}{\omega_2}\right) = -(\varepsilon_L - 1)\,\frac{\int_{V_L} \vec{E}_1 \cdot \vec{E}_2 dV}{\int_{V_c} \vec{E}_1 \cdot \vec{E}_2 dV} \quad . \qquad (6b)$$

For $\varepsilon_L \approx 1$, we write this equation as

$$\frac{\omega_2 - \omega_1}{\omega_2}\left(1 + \frac{\omega_1}{\omega_2}\right) \approx -(\varepsilon_L - 1)\,\frac{\int_{V_L} E_1^2 dV}{\int_{V_c} E_1^2 dV} \quad ; \qquad (7b)$$

this equation should extend the range of validity around $\varepsilon_L = 1$ of Eq. (7a), since (7b) is exact for the limiting cases $V_L \to 0$ and $V_L = V_c$.

Finally it should be pointed out that it the frequency shift is measured respect to the frequency corresponding to full tank conditions, we would have

$$\frac{\omega_1^2}{\omega_2^2} = 1 - \frac{\varepsilon_L - 1}{\varepsilon_L}\,\frac{\int_{V_v} \vec{E}_1 \cdot \vec{E}_2 dV}{\int_{V_c} \vec{E}_1 \cdot \vec{E}_2 dV} \qquad (6c)$$

$$\frac{\omega_1'^2}{\omega_2^2} = 1 - \frac{\varepsilon_L - 1}{\varepsilon_1} \frac{\int_{V_v} E_1^2 dV}{\int_{V_c} E_1^2 dV} \qquad (7c)$$

where $V_v = V_c - V_L$ (the volume occupied by the propellant vapor) and $\omega_1' = \omega_1/\varepsilon_L^{1/2}$ is obviously the frequency corresponding to a full tank condition.

III.2 *FREQUENCY SHIFT FOR ε_L CLOSE TO UNITY*

Equation (6b) clearly shows that the frequency shift, $\omega_2-\omega_1$, does depend on the liquid configuration. To determine that dependency would be a quite difficult task because in the integral $\int_{V_L} \vec{E}_1 \cdot \vec{E}_2 dV$ not only the region of integration V_L, but $\vec{E}_2$ itself, will depend on the particular configuration existent.

A case for which the determination of that dependency becomes quite simple is the limit $\varepsilon_L \simeq 1$, since Eq.(7b) does not involve $\vec{E}_2$, and for relatively simple cavity geometries $\vec{E}_1$ can be obtained once a resonant mode is selected.

This limiting case has the additional advantage that for particular resonant modes (perhaps not the fundamental one), the integral $\int_{V_L} \vec{E}_1^2 dV$ can be shown to be weakly dependent on the configuration of V_L. On the other hand for ε_L not too close to unity, $\vec{E}_2$ will certainly depend on the liquid configuration, so that it appears impossible to make $\int_{V_L} \vec{E}_1 \cdot \vec{E}_2 dV$ independent of the configuration, by selecting a particular resonant mode $\vec{E}_1$.

It is fortunate that for our case ε_L is not far from unity (Table II), so that Eq.(7b) can be approximately substituted for Eq.(6b). It is convenient nevertheless to improve upon Eq.(7b) by carrying out an expansion of $\vec{E}_2$ in powers of ε_L-1, and retaining terms beyond the lowest one in Eq. (6b).

To this end, let us consider the tank empty. By taking the rotor of Eq.(1) and using Eq.(2) and equation

$$\nabla . \vec{E} = 0 \quad , \tag{12}$$

we get

$$\nabla (\nabla.\vec{E}) - \nabla^2\vec{E} = -\nabla^2\vec{E} = \omega^2\mu_o\varepsilon_o\vec{E} \quad . \tag{13}$$

The equation

$$\nabla^2\vec{E} + \lambda\vec{E} = 0 \tag{14}$$

(where $\lambda \equiv \omega^2\mu_o\varepsilon_o$) for an arbitrary cavity, with boundary conditions at the walls

$$\vec{n} \wedge \vec{E} = 0 \tag{15}$$

(n being the normal to the wall) and the auxiliary condition Eq. (12) is known to have a discrete, numerable spectrum of eigen values λ_n and eigen-functions $\vec{E}_n$, such that

$$\nabla^2\vec{E}_n + \lambda_n\vec{E}_n = 0 \quad , \quad n = 1, 2, \cdots ; \tag{16}$$

$\omega_n^2 = \lambda_n/\mu_o\varepsilon_o$ is the frequency of the n^{th} resonant mode $\vec{E_n}$.

Since Eqs.(12), (15) and (16) are homogeneous, $\vec{E}_n$ can be normalized:

$$\int_{V_c} \vec{E}_n^2 \, dV = 1 \quad . \tag{17}$$

On the other hand we have

$$\int_{V_c} \vec{E}_n \cdot \vec{E}_m dV = 0 \quad , \quad n \neq m \quad . \tag{18}$$

To show this we multiply Eq.(16) by $\vec{E}_m$ and integrate over the volume of the cavity V_c

$$\int_{V_c} \vec{E}_m \cdot (\nabla^2 \vec{E}_n) dV + \lambda_n \int_{V_c} \vec{E}_m \cdot \vec{E}_n dV =$$

$$= \int_{V_c} \nabla \cdot (\vec{E}_m \cdot \nabla \vec{E}_n) dV - \int_{V_c} \nabla \vec{E}_m : \nabla \vec{E}_n dV + \lambda_n \int_{V_c} \vec{E}_m \cdot \vec{E}_n dV = 0. \quad (19)$$

$\vec{E}_m \cdot \nabla \vec{E}_n$ inside the third integral above is the product of the vector $\vec{E}_m$ with the tensor $\nabla \vec{E}_n$; $\nabla \vec{E}_m : \nabla \vec{E}_n$ is the tensor product of $\nabla \vec{E}_m$ and $\nabla \vec{E}_n$. Similarly we get

$$\int_{V_c} \nabla \cdot (\vec{E}_n \cdot \nabla \vec{E}_m) dV - \int_{V_c} \nabla \vec{E}_n : \nabla \vec{E}_m dV + \lambda_m \int_{V_c} \vec{E}_n \cdot \vec{E}_m dV = 0. \quad (20)$$

The difference between Eqs.(19) and (20) yields

$$(\lambda_m - \lambda_n) \int_{V_c} \vec{E}_n \cdot \vec{E}_m dV = \int_{V_c} \nabla \cdot (\vec{E}_m \cdot \nabla \vec{E}_n - \vec{E}_n \cdot \nabla \vec{E}_m) dV \equiv \int_{\Sigma_c} d\vec{\Sigma} \cdot (\vec{E}_m \cdot \nabla \vec{E}_n - \vec{E}_n \cdot \nabla \vec{E}_m). \quad (21)$$

Using Eq.(15) the surface integral becomes

$$\int_{\Sigma_c} d\Sigma \left[E_{mN} \frac{E_{nN}}{\partial N} - E_{nN} \frac{E_{mN}}{\partial N} \right] \quad (22)$$

that vanishes because from Eqs. (12) and (15) ,

$$\frac{\partial E_{nN}}{\partial N} \propto E_{nN} \quad , \quad \frac{\partial E_{mN}}{\partial N} \propto E_{mN} \quad (23)$$

where the proporcionality factor depends only on the local geometry of the wall; $\partial/\partial N$ is the derivative along the normal to the wall

and E_{nN} , E_{mN} are the normal components of $\vec{E}_n$, $\vec{E}_m$ at the wall.

Under very general conditions the orthonormal system of eigen-functions $\{\vec{E}_n\}$ is complete, so that any vector function $\vec{A}$ satisfying condition $\vec{A}_t = 0$ at the cavity walls and the auxiliary condition $\nabla \cdot \vec{A} = 0$, can be expanded as a series in terms of $\{\vec{E}_n\}$; $n = 1, 2, - - - .$

It is evident that when the cavity is completely full,the eigenvalues will be $\lambda'_n = \lambda_n/\varepsilon_L$; obviously $\vec{E}'_n \equiv \vec{E}_n$.

Let us now consider that the cavity (tank) is partially filled. The best way to proceed is to assume that the transition of the dielectric constant ε across a vapor-liquid interface is not discontinuous, but varies continuously through a thin layer from 1 well inside the vapor to ε_L well inside the liquid; in the results the case of interest here is recovered by letting the thickness of that transition layer become vanishingly small.

Then instead of Eq.(12) we will have

$$\nabla \cdot \varepsilon\vec{E} = 0$$

or
$$\nabla \cdot \vec{E} = -\vec{E} \cdot \nabla \ln\varepsilon \quad , \tag{12'}$$

so that instead of Eq.(14) we will have

$$\nabla^2\vec{E} + \nabla(\vec{E} \cdot \nabla \ln\varepsilon) + \varepsilon\lambda\vec{E} = 0 \quad . \tag{14'}$$

Equation (15) remains unchanged.

For $\varepsilon \to 1$, Eqs.(12') and Eqs.(14') go into (12) and (14). For $\varepsilon \neq 1$ the eigenfunctions $\vec{E}_n^*$ and eigenvalues λ_n^* will be very close to $\vec{E}_n$ and λ_n. Writing

$$\vec{E}_n^* = \vec{E}_{no} + \vec{E}_{n1} + \vec{E}_{n2} + \ldots \tag{24}$$

$$\lambda_n^* = \lambda_{no} + \lambda_{n1} + \lambda_{n2} + \ldots \tag{25}$$

where $\vec{E}_{no} = \vec{E}_n$, $\lambda_{no} = \lambda_n$, and E_{ni} and λ_{ni} are of order of δ^i (δ being ε-1), Eqs.(14'), (12') and (15) produce

$$\begin{aligned}
&\nabla^2\vec{E}_{no} + \lambda_{no}\vec{E}_{no} = 0 \quad , \\
&\nabla^2\vec{E}_{n1} + \lambda_{no}\vec{E}_{n1} + \lambda_{n1}\vec{E}_{no} + \lambda_{no}\delta\vec{E}_{no} + \nabla(\vec{E}_{no}\cdot\nabla\delta) = 0 \quad , \\
&\nabla^2\vec{E}_{n2} + \lambda_{no}\vec{E}_{n2} + \lambda_{n1}\vec{E}_{n1} + \lambda_{n2}\vec{E}_{no} + \lambda_{n1}\delta\vec{E}_{no} \\
&\quad + \lambda_{no}\delta\vec{E}_{n1} + \nabla(\vec{E}_{n1}\cdot\nabla\delta) - \frac{1}{2}\nabla(\vec{E}_{no}\cdot\nabla\delta^2) = 0
\end{aligned} \tag{26}$$

(and similar equations for i = 3, 4, ...);

$$\begin{aligned}
\nabla\cdot\vec{E}_{no} &= 0 \quad , \\
\nabla\cdot\vec{E}_{n1} &= -\vec{E}_{no}\cdot\nabla\delta \quad , \\
\nabla\cdot\vec{E}_{n2} &= -\vec{E}_{n1}\cdot\nabla\delta + \frac{1}{2}\vec{E}_{no}\cdot\nabla\delta^2
\end{aligned} \tag{27}$$

(and similar equations for i = 3, 4, ...);

$$\vec{n} \wedge \vec{E}_{ni} = 0 \quad , \quad i = 0; 1, 2, \ldots \tag{28}$$

It is clear that $\vec{E}_{n_i}$ (i = 1, 2, ...) does not satisfy Eq. (12), so that $\vec{E}_{n_i}$ (i = 1, 2, ...) can not be expanded in a series of the eigenfunctions for the empty cavity, $\{\vec{E}_n\}$. Nevertheless, since any vector function can be expressed in terms of the gradient of a scalar and a divergence-free vector, we can write

$$\vec{E}_{n_i} = \nabla\psi_i + \vec{\Gamma}_i \quad , \quad \nabla \cdot \vec{\Gamma}_i = 0 \; . \tag{29}$$

and therefore, from (27) and (26) we have

$$\begin{aligned} \nabla^2\psi_1 &= -\vec{E}_n \cdot \nabla\delta \; , \\ \nabla^2\psi_2 &= -\left(\nabla\psi_1 + \vec{\Gamma}_1\right) \cdot \nabla\delta + \frac{1}{2}\,\vec{E}_n \cdot \nabla\delta^2 \end{aligned} \tag{30}$$

and

$$\begin{aligned} &\nabla^2\vec{\Gamma}_1 + \lambda_n\vec{\Gamma}_1 + \lambda_n\left(\delta\vec{E}_n + \nabla\psi_1\right) + \lambda_{n1}\vec{E}_n = 0 \quad , \\ &\nabla^2\vec{\Gamma}_2 + \lambda_n\vec{\Gamma}_2 + \lambda_n\left(\nabla\psi_2 + \delta\vec{\Gamma}_1 + \delta\nabla\psi_1\right) + \lambda_{n1}\left(\vec{\Gamma}_1 + \delta\vec{E}_n + \nabla\psi_1\right) + \lambda_{n2}\vec{E}_n = 0 \end{aligned} \tag{31}$$

Equations (30) are to be solved with the boundary conditions

$$\vec{n} \wedge \nabla\psi_i = 0 \tag{32}$$

at the walls, or equivalently, ψ_i = constant at the walls. Since

$\vec{\Gamma}_i$ satisfies Eq.(12) and is tangent to the walls, it can be expanded in $\{\vec{E}_n\}$. We thus write

$$\vec{\Gamma_1} = \sum_p \alpha_p \vec{E}_p \quad , \tag{33}$$

and then

$$\sum_p \alpha_p (\lambda_n - \lambda_p) \vec{E}_p + \lambda_n (\delta\vec{E}_n + \nabla\psi_1) + \lambda_{n1}\vec{E}_n = 0 \quad . \tag{34}$$

Multiplying Eq.(34) by $\vec{E}_m$ and integrating over the entire cavity, we get

$$\alpha_m(\lambda_n - \lambda_m) + \lambda_{n1}\int_{V_c} \vec{E}_m \cdot \vec{E}_n dV + \lambda_n \int_{V_c} (\delta\vec{E}_m \cdot \vec{E}_n + \vec{E}_m \cdot \nabla\psi_1) dV = 0 \tag{35}$$

For $m = n$, we get

$$\lambda_{n1} = - \lambda_n \delta_L \int_{V_L} \vec{E}_n^2 dV \quad , \tag{36}$$

where we have used the result

$$\int_{V_c} \vec{E}_n \cdot \nabla\psi_1 dV \equiv \int_{V_c} \nabla\cdot(\vec{E}_n\psi_1) dV - \int_{V_c} (\nabla\cdot\vec{E}_n)\psi_1 dV =$$

$$= \int_{\Sigma_c} \psi_1 \vec{E}_n \cdot d\vec{\Sigma} \propto \int_{\Sigma_c} \vec{E}_n \cdot d\vec{\Sigma} = 0 \quad .$$

For $m \neq n$, we get

$$\alpha_m = \frac{\lambda_n}{\lambda_m - \lambda_n} \delta_L \int_{V_L} \vec{E}_m \cdot \vec{E}_n dV \quad . \tag{37}$$

We can set $\alpha_n = 0$, by requiring normalization of $\vec{E}_n^*$ to order δ ,

that is

$$1 = \int_{V_c} (\vec{E}_n^*)^2 dV \simeq \int_{V_c} \vec{E}_n^2 dV + 2 \int_{V_c} \vec{E}_n \cdot (\nabla\psi_1 + \Sigma\alpha_p \vec{E}_p) dV = 1 + 2\alpha_n .$$

Multiplying the second Eq.(31) by $\vec{E}_n$ and integrating over the cavity we get

$$\lambda_{n2} + \lambda_{n1}\delta_L \int_{V_L} \vec{E}_n^2 dV + \lambda_n \int_{V_c} dV \vec{E}_n \cdot \left[\delta\vec{\Gamma}_1 + \delta\nabla\psi_1\right] = 0$$

so that finally

$$\lambda_n^* = \lambda_n \left[1 - \delta_L \int_{V_L} \vec{E}_n^2 dV + \delta_L^2 \int_{V_L} \vec{E}_n^2 dV - \delta_L^2 \sum_{p\neq n} \frac{\left(\int_{V_L} \vec{E}_n \cdot \vec{E}_p dV\right)^2}{(\lambda_p/\lambda_n) - 1} - \delta_L \int_{V_L} dV\, \vec{E}_n \cdot \nabla\psi_1 + O(\delta_L^3)\right] .$$

Substituting back ω^2 for $\lambda/\mu_o\varepsilon_o$, we obtain

$$(\omega_n^*)^2 = \frac{\omega_n^2}{1+\delta_L x} \left[1 + \frac{\delta_L\left(x - \int_{V_L} \vec{E}_n^2 dV\right)}{1 + \delta_L \int_{V_L} \vec{E}_n^2\, dV} - \delta_L^2 \sum_{p\neq n} \frac{\left(\int_{V_L} \vec{E}_p \cdot \vec{E}_n dV\right)^2}{(\omega_p/\omega_n)^2 - 1} - \delta_L^2 \int_{V_L} dV\, \vec{E}_n \cdot \nabla\phi_1 + O(\delta_L^3)\right] \qquad (38)$$

where

$$\nabla^2\phi_1 = -\vec{E}_n \cdot \nabla(\delta/\delta_L) ,$$

and ϕ_1 is a constant at the walls. This constant can be chosen to be zero. Then we have

$$\phi_1 = \frac{1}{4\pi} \int_{V_c} G_D \nabla \cdot \left(\frac{\delta}{\delta_L} \vec{E}_n\right) dV \qquad (38')$$

where G_D is the Green function for Laplace's equation inside the cavity, with Dirichlet conditions.

Calling the last bracket in (38) $1 + \Delta$, we get*

$$\frac{V_L}{V_c} \equiv x = \frac{(\omega_n/\omega_n^*)^2 - 1}{\delta_L} + \frac{\omega_n^2}{\delta_L(\omega_n^*)^2}\,\Delta \quad . \tag{39}$$

If the last term can be neglected above, V_L can be deduced by measuring ω_n^* (the resonant frequency of the selected mode at the desired time) and using Eq.(39). It is clear that the error of the measurement is due to the fact that, in general, Δ does not vanish and depends on the (unknown) configuration.

---

* Using the symbols of Sec. III-1, $\omega_n \equiv \omega_1$, $\omega_n^* \equiv \omega_2$, and $\vec{E}_n = \vec{E}_1$, $\vec{E}_n^* = \vec{E}_2$.

III-3 *DISCUSSION OF THE MEASUREMENT ERROR*

A) *General Considerations*

The analysis of the last section yields Eq.(39) for x . If one takes the approximation

$$x \simeq \left[(\omega_n/\omega_n^*)^2 - 1\right]\delta_L^{-1} \tag{40}$$

as the value predicted by the analysis, the resulting error is

$$\text{Error } (x) = \frac{\omega_n^2 \Delta}{(\omega_n^*)^2 \delta_L} \simeq x\left(1 - \frac{\int_{V_L} \vec{E}_n^2 \, dV}{x}\right)$$

$$-\delta_L \sum_{p \neq n} \frac{\left(\int_{V_L} \vec{E}_p \cdot \vec{E}_n dV\right)^2}{(\omega_p/\omega_n)^2 - 1} - \delta_L \int_{V_L} \vec{E}_n \cdot \nabla\phi_1 dV \; . \tag{41}$$

$\left|\text{Error } (x)\right|$ vanishes, of course, for x = 0 and x = 1, and will reach maxima not near to the ends of the range $0 \leq x \leq 1$.

In the general specifications of this study a maximum error in the determination of propellant content, of 2% of full scale, was established as desirable. It is clear however that such accuracy is really necessary when the tank is far from being full. To make definite the discussion we shall require below that $\left|\text{Error } (x)\right|$ in (41) be less than 0.02 for $x \leq 0.10$, and less than 0.05 for x = 0.50.

For δ_L sufficiently small the last two terms in Eq.(41) can be discarded. How small δ_L has to be in this respect, must be verified in every particular problem; such verification is not greatly difficult, however, for tanks with shapes that not differ greatly from relatively simple geometries, as it will be seen below for the Shuttle case. Then, the error bounds above indicated imply the following conditions:

$$\left| x\left(1 - \frac{\int_{V_L} \vec{E}_n^2 dV}{x} \right) \right| \begin{array}{ll} < 0.02 \quad , & (x = 0.10) \\ < 0.05 \quad , & (x=0.50) \quad , \end{array} \tag{42}$$

or equivalently,

$$0.80 < \frac{\int_{V_L} \vec{E}_n^2 dV}{V_L} \Big/ \frac{\int_{V_c} \vec{E}_n^2 dV}{V_c} < 1.20 \quad , \quad (V_L = 0.10\ V_c)$$

$$0.90 < \frac{\int_{V_L} \vec{E}_n^2 dV}{V_L} \Big/ \frac{\int_{V_c} \vec{E}_n^2 dV}{V_c} < 1.10 \qquad (V_L = 0.50\ V_c) \ . \tag{43}$$

The meaning of these requirements is that the mean value of $\vec{E}_n^2$ over the liquid region must be close, within certain bounds, to the mean value $\vec{E}_n^2$ over the entire tank. Obviously such require-

ments are, in general, the easier to satisfy, the larger the value of n , since the eigenfunction $\vec{E}_n$ becomes more complicated (it has more nodes) as n increases. There are, however, limitations on the magnitude of n , because the resonant frequencies become too crowded for n large enough. For every particular problem, a suitable mode (ω_n and $\vec{E}_n$) should be selected; the way to carry out this, will be illustrated below, for the Shuttle case.

B) *The Shuttle Case*

We will first study in detail the case of the small LOX tank (see Fig.1). The first step of the analysis is to determine the eigenfrequencies and eigenfunctions, ω_n and $\vec{E}_n$, of the tank, so that a suitable resonant mode can be selected. In most cases, the tank shape can be approximated by a relatively simple geometry so that ω_n and $\vec{E}_n$ can be calculated analytically and the general characteristics of any mode can be approximately determined.(Nevertheless, the present method can also be applied to complicated tank shapes, by measuring experimentally the characteristics of the resonant modes). It should be understood that the value of ω_n used in Eq.(39) should be found experimentally by identifying in practice the mode selected analytically, the real and the theoretical modes having very similar characteristics, because, as it is well known, the eigenfunctions and eigenvalues of Helmholtz's

equation (14), for two cavities that differ little from each other, are approximately the same |8| .

The LOX tank considered can be approximated by a cylinder of R = 1.0 m. radius and L = 2.00 m. length. The resonant modes of a cylindrical cavity are well known |9| . There are two kinds of modes, TM and TE modes. Their eigenfrequencies and eigenfunctions are:

$$\text{TM} \quad \begin{cases} \omega = \dfrac{1}{(\mu_o \varepsilon_o)^{1/2}} \left(\dfrac{x_{\alpha\beta}^2}{R^2} + \dfrac{\pi^2 \gamma^2}{L^2} \right)^{1/2} \\ E_z = K \cos\left(\dfrac{\pi\gamma z}{L}\right) J_\alpha \left(x_{\alpha\beta} \dfrac{r}{R}\right) \begin{Bmatrix} \cos \alpha\phi \\ \operatorname{sen} \alpha\phi \end{Bmatrix} \\ \vec{E}_\perp = -K \dfrac{\pi\gamma R^2}{L x_{\alpha\beta}^2} \sin\left(\dfrac{\pi\gamma z}{L}\right) \nabla_\perp \left[J_\alpha \left(x_{\alpha\beta} \dfrac{r}{R}\right) \begin{Bmatrix} \cos \alpha\phi \\ \operatorname{sen} \alpha\phi \end{Bmatrix} \right], \end{cases} \tag{44}$$

$$\text{TE} \quad \begin{cases} \omega = \dfrac{1}{(\mu_o \varepsilon_o)^{1/2}} \left(\dfrac{x'^2_{\alpha\beta}}{R^2} + \dfrac{\pi^2 \gamma^2}{L^2} \right)^{1/2}, \\ E_z = 0, \\ \vec{E}_\perp = K' \sin\left(\dfrac{\pi\gamma z}{L}\right) \vec{u}_z \wedge \nabla_\perp \left[J_\alpha \left(x'_{\alpha\beta} \dfrac{r}{R}\right) \begin{Bmatrix} \cos \alpha\phi \\ \operatorname{sen} \alpha\phi \end{Bmatrix} \right], \end{cases}$$

where E_z and $\vec{E}_\perp$ are the components of the electric field parallel and transverse to the cylinder axis; $\vec{u}_z$ is a unit vector along that axis; $\nabla_\perp$ is the transverse gradient; z,r and ϕ are defined in Fig.II; K and K' are normalizing constants; J_α is the Bessel function of the first kind and α order; $x_{\alpha\beta}$ and $x'_{\alpha\beta}$ are the β zero of $J_\alpha(x_{\alpha\beta}) = 0$ and $J'_\alpha(x'_{\alpha\beta}) = 0$ respectively, and γ is an integer number.

It is obvious that if the electric field were constant in space, the first term in Eq.(41), would vanish. In our case,the mode that best approaches that condition, is a TM mode with $\alpha = \gamma = 0$. To make the experimental identification of such a mode easier, we choose $\beta = 1$, so that our $\vec{E}_n$ will be

$$\vec{E}_n = \vec{u}_z K J_o(x_{01}\, r/R) \ . \qquad (46).$$

We can now discuss quantitatively the error of the measurement. Let us, first, assume that the last two terms of Eq.(41) can be neglected. There are two limit situations in weightlessnes conditions:

1) When accelerations are small, the liquid-vapor configuration is governed by surface tension effects. The contact angle of LOX is known to be close to zero (perfectly wetting liquid). As it is well known, for such liquids, the liquid-vapor interface

is a constant-curvature surface, concave toward the vapor phase |10| . It is clear that for this tank, the propellant will adopt almost always the configuration shown in Fig.III (a), as long as its volume lies between 16.7% and 66.7% of the total volume,

$$\frac{R}{3L} < x < 1 - \frac{2R}{3L} \tag{47}$$

Writing Error (x) = $\Omega_1 + \Omega_2$, where Ω_1 is the first term on the right side of (41), and Ω_2 is the sum of the other two terms, we will have

$$\Omega_1 = \frac{V_L}{V_c} - \int_{V_L} \vec{E}_n^2 \, dV$$

$$= \frac{V_1}{V_c} - \frac{V_2}{V_c} - \int_{V_1} \vec{E}_n^2 \, dV + \int_{V_2} \vec{E}_n^2 \, dV$$

$$= \int_{V_2} \vec{E}_n^2 \, dV - \frac{V_2}{V_c} \quad , \tag{48}$$

where V_1 is the volume of that part of the tank below the M-N section, and V_2 is that part of V_1 occupied by the vapor (which is a hemisphere of radius R); the first and third terms in the second line of Eq.(48) balance each other, since $\vec{E}_n$ does dot depend on z . Inserting (46) in (47) we get

$$\int_{V_2} \vec{E}_n^2 \, dV - V_2/V_c \equiv \frac{\int_0^{2\pi} d\phi \int_0^R r dr J_o^2(x_{o1} r/R) \sqrt{R^2 - r^2}}{\int_0^{2\pi} d\phi \int_0^R r dr J_o^2(x_{01}\, r/R)\, L}$$

$$- \frac{2\pi R^3/3}{\pi R^2 L} \simeq 0.424 - 0.333 \simeq 0.09 \quad , \tag{49}$$

by numerical integrations, and substitution of the values of x_{01}, R and L.

It is clear that Ω_1 is independent of the liquid content for the range given in Eq.(47). When x becomes smaller than 0.167, Ω_1 will decrease as it is easy to verify [the volume V_2 in (48) becomes smaller than a hemisphere, while it gets closer to V_1].

2) When accelerations are dominant, the liquid will adopt a configuration, of the type shown in Fig.IV, that is, with a plane liquid-vapor interface. For configuration (a) of this figure Ω_1 vanishes. As the angle between the cylinder axis and the normal to the interface plane is increased, Ω_1 remains, obviously, zero until configuration (b) is reached. When that angle increases further and the tank is 10% filled, it is clear that Ω_1 becomes positive and reaches a maximum when the liquid adopts the limiting case (d). If the tank is 50% filled, Ω_1 remains always zero. The maximum of Ω_1 for x = 0.1 is easy to calculate. We have

$$\Omega_1 = x - \frac{\int_{r_c}^{R} r dr J_o^2(x_{01} r/R) 2\int_{o}^{\phi(r)} d\phi}{\int_{o}^{R} r dr\, J_o^2(x_{01}\, r/R) \int_{o}^{2\pi} d\phi} \simeq 0.1 - 0.021 = 0.079 \quad , \quad (50)$$

where $\phi(r) = \cos^{-1}(r_c/r)$ and $r_c = 0.69\ R$ [see Fig.IV(d)].

Let us now consider Ω_2 . This quantity is very easy to compute for configuration (a) of Fig.IV. We first need to explicitly obtain Ω_2 . From Eq.(38') we get

$$\Phi_1(\vec{r}) = -(4\pi)^{-1} \int_{V_L} \vec{E}_n(\vec{r}') \cdot \nabla' G_D(\vec{r},\vec{r}')dV' \qquad (51)$$

so that Ω_2 becomes

$$\Omega_2 = -\delta_L \sum_{p\neq n} \frac{\left(\int_{V_L} \vec{E}_p \cdot \vec{E}_n dV\right)^2}{(\omega_p/\omega_n)^2 - 1} + \frac{\delta_L}{4\pi} \int_{V_L} dV \int_{V_L} dV' \vec{E}_n(\vec{r}) \vec{E}_n(\vec{r}') : \nabla\nabla' G_D(\vec{r},\vec{r}'), \qquad (52)$$

As it is well known, Green's function for a cylinder with Dirichlet conditions is [9]

$$G_D(\vec{r},\vec{r}') = \frac{8}{LR^2} \sum_{\alpha=-\infty}^{\infty} \sum_{\beta=1}^{\infty} \sum_{\gamma=1}^{\infty} e^{i\alpha(\phi-\phi')} \sin\left(\frac{\gamma\pi z}{L}\right) \sin\left(\frac{\gamma\pi z'}{L}\right)$$

$$J_\alpha(x_{\alpha\beta} r/R)\, J_\alpha(x_{\alpha\beta} r'/R) \left[\left(\frac{x_{\alpha\beta}}{R}\right)^2 + \left(\frac{\gamma\pi}{L}\right)^2\right]^{-1} \left[J_{\alpha+1}(x_{\alpha\beta})\right]^{-2} . \qquad (53)$$

After long and tedious manipulations, (52) can be written as

$$\Omega_2 = \delta_L \sum_{p\neq n} \left(\int_{V_L} E_n \hat{E}_{pz} dV\right)^2 \left[1 + \frac{x_{\alpha\beta}^2/R^2}{(\pi\gamma/L)^2-(x_{01}/R)^2}\right]^{-1} , \qquad (54)$$

where we used the fact that $\vec{E}_n \equiv \hat{u}_z E_n$, so that only the TM modes contribute to the series in the first term of (52); the p-index represents the p^{th} combination of the α , β and γ indices, and E_{pz} has been renormalized to have $\int_{V_c} E_{pz}^2 dV = 1$.

For configuration (a) in Fig.IV,

$$\int_{V_L} E_n E_{pz} dV \propto \int_o^R J_o(x_{01} r/R) J_\alpha(x_{\alpha\beta} r/R) \int_o^{2\pi} d\phi \begin{Bmatrix} \cos \alpha\phi \\ \sin \alpha\phi \end{Bmatrix} \qquad (55)$$

so that only the $\alpha = 0$, $\beta = 1$ values need be considered in (54). Then we have

$$\Omega_2 = \delta_L \sum_{\gamma=1}^{\infty} \frac{\left[2\pi \int_o^R r dr J_o^2(x_{01}\, r/R) \int_o^{xL} dz \cos(\pi\gamma z/L)\right]^2}{2\pi L \int_o^R r dr J_o^2(x_{01} r/R) 2\pi (L/2) \int_o^R r dr J_o^2(x_{01} r/R)} \left[1-\left(\frac{x_{01} L}{\pi\gamma R}\right)^2\right]$$

$$= 2\delta_L \sum_{\gamma=1}^{\infty} \left[\frac{\text{sen}\ (\pi\gamma x)}{\pi\gamma}\right]^2 \left[1 - \left(\frac{x_{01} L}{\pi\gamma R}\right)^2\right]$$

$$\simeq -\delta_L x(1-x)\left[\left(\frac{x_{01} L}{R}\right)^2 \frac{x(1-x)}{3} - 1\right] \simeq - \frac{x(1-x)}{2}\left[7.71\, x\,(1-x) - 1\right] . \qquad (56)$$

The maximum of $|\Omega_2|$ in (56) occurs for $x = 1/2$,

$$\Omega_2 \ (x=1/2) \simeq -0.11. \qquad (57)$$

The reason why $|\Omega_2|$ reaches such a relatively large value is that obviously the configuration of Fig.IV(a) brings in modes that are z-dependent ($\gamma \neq 0$), with α and β the same of the selected mode ($\alpha=0$, $\beta=1$); for such modes the quantity inside the bracket in Eq. (54) is small (a nearly-resonant effect). On the contrary, for configuration IV (d), only modes with $\gamma = 0$ are brought in, so that there is no such effect and Ω_2 will be much smaller. Configurations like IV(b) and IV(c) will present Ω_2 values that lie between those extremes; for configuration III(a), Ω_2 will be close to the value for IV(a).

In setting Error (x) = $\Omega_1 + \Omega_2$ in Eq.(41) we neglected terms $0(\delta_L^2)$. Since $\Omega_1 = 0$ for Fig.IV(a), and $|\Omega_2|$ can reach up to 0.11, it would be convenient to calculate the terms $0(\delta_L^2)$. In fact, for such configuration, it is possible to exactly calculate ω_n^* , and thus find out the importance of the terms $0(\delta_L^2)$ and beyond. To this end the equation

$$\nabla^2 E_{nz}^* + \lambda_n^* \varepsilon E_{nz}^* = 0$$

with $\varepsilon = \varepsilon_L$ in the liquid and $\varepsilon = 1$ in the vapor, must be solved with boundary conditions $E_{nz}^* = 0$ at $r = R$, $\partial E_{nz}^*/\partial z = 0$ at $z = 0$, L, and the usual conditions for the interface of two dielectrics satisfied at $z = xL$. After cumbersome transformations, we get

$$\tan\left[x(y\varepsilon_L-1)^{1/2}Lx_{01}/R\right] = \varepsilon_L\left[(1-y)/(y\varepsilon_L-1)\right]^{1/2}\tanh\left[(1-x)\right.$$

$$\left.\times\,(1-y)^{1/2}Lx_{01}/R\right] \qquad (58)$$

where $y = (\omega_n^*/\omega_n)^2$. This equation gives y as a function of x , and may be compared with Eq.(40), that is,

$$y = (1+\delta_L x)^{-1} \quad . \qquad (59)$$

For x = 0.43 we find from (58) that the error of Eq.(59) is Error (x) = -0.07, and for x = 0.19, Error (x) = -0.01. It is clear that retaining terms $0(\delta_L^2)$ in Error (x) reduces the error.

As it can be seen, the measurement errors, although reasonable, exceed somewhat in some cases the error bounds previously suggested. It should be noted, however, that the selected mode is the fundamental one, that is, it has the lowest frequency of all modes; this makes mode detection extremely simple. It is clear that if one would have chosen a higher mode, the error of formula (40) would decrease.

Let us now consider the larger LH_2 tank (Fig.1). This tank can be approximated by a cylinder of length L = 20.3 m and radius R = 2.1 m. The first point to note is that for such large L/R ratios, the "resonant" effect previously noticed when discussing

the Ω_2 term, becomes quite large [see Eq.(56)] . To avoid this, we select the first TE mode, which has $\alpha = 1$, $\beta = 1$, $\gamma = 1$. This mode has a z-dependency, so that the above effect is much less important. For such large L/R ratios this TE mode is the fundamental one, as can be seen from Eq.(44).

We first consider the case when accelerations are dominant. For the configuration of Fig.IV(a) we have for Ω_1

$$\Omega_1 = x - \left[\int_0^{xL} dz \sin^2(\pi z/L)\right]\left[\int_0^{L} dz \sin^2(\pi z/L)\right]^{-1} = (\sin 2\pi x)/2\pi. \qquad (60)$$

For the configuration of Fig.IV(d) we have $\Omega_1 = 0$ for $x = 0.5$, and for $x = 0.1$

$$\Omega_1 = x - \frac{\int_{r_c}^{R} r dr \, 2\int_0^{\phi(r)} d\phi \left[\left\{\frac{J_1(x'_{11} r/R)}{r}\sin\phi\right\}^2 + \left\{\frac{x'_{11} J'_1(x'_{11} r/R)}{R}\cos\phi\right\}^2\right]}{\int_0^{R} r dr \int_0^{2\pi} d\phi \left[\left\{\frac{J_1(x'_{11} r/R)}{r}\sin\phi\right\}^2 + \left\{\frac{x'_{11} J'_1(x'_{11} r/R)}{R}\cos\phi\right\}^2\right]} \qquad (61)$$

where $r_c = 0.69R$, and $\phi(r) = \cos^{-1}(r_c/r)$; then

$$\Omega_1 = 0.1 - 0.022 = 0.078.$$

For configuration IV(a), Ω_2 can be calculated as in the case of the small LOX tank, but it is as simple to compute exactly Error(x). Following a mathematical development quite similar to the one leading to Eq.(58), we obtain

$$\tan\left[x(\varepsilon_L y'-1)\ \frac{Lx'_{11}}{R}\right] \simeq -\left(\frac{\varepsilon_L y'-1}{y'-1}\right)^{1/2} \tan\left[(1-x)(y'-1)^{1/2}\ \frac{Lx'_{11}}{R}\right] \quad (62)$$

where $y' = (\omega_n^*/\omega_n)^2\left[1 + (\pi R/Lx'_{11})^2\right]$, and when $y' < 1$, the right-hand side of Eq.(62) should be

$$-\left(\frac{\varepsilon_L y'-1}{1-y'}\right)^{1/2} \tan\left[(1-x)(1-y')^{1/2}\ \frac{Lx'_{11}}{R}\right] \quad ;$$

for $x = 0.208$, Error $(x) \simeq 0.067$, and for $x = 0.30$, Error$(x) = -0.073$. For the configuration of Fig.IV(d), Ω_2 is negligible.

For the configuration of Fig.III(a), Error (x) is close to its value for case IV(a). It can be verified that the error for configurations III(b) and (c) is smaller.

The analysis for the other two tanks, is identical to the preceding one. For all these three tanks, the error can be decreased by choosing higher modes, as in the case of the small LOX tank.

III.4 COMPUTATION OF RESONANT FREQUENCIES, RESPONSE TIME AND POWER CONSUMPTION

For the tanks considered in detail in Sec.III.3, Eqs.(44) and (45) give the frequencies of the selected modes

$$\omega\ (\mathrm{LOX}) = 722\ \mathrm{MHz}\quad ,$$
$$\omega\ (\mathrm{LH_2}) = 267\ \mathrm{MHz}\quad . \tag{63}$$

For the computation of the time response of the gaging system it is necessary to previously calculate the Q-factors of the tanks. From Ref.|9|, we have

$$Q(\mathrm{LOX}) = \frac{1}{2\pi}\,\frac{L}{S}\,\frac{1}{1 + L/R} \tag{64}$$

where S is the skin depth,

$$S = C(2\pi\omega\sigma)^{-1}\quad , \tag{65}$$

and σ is the electrical conductivity of the tank walls. We also have

$$Q(\mathrm{LH_2}) = \frac{1}{4\pi}\,\frac{L}{S}\,\frac{1 + 0.344\ L^2/R^2}{1 + 0.209\ L/R + 0.242\ L^3/R^3}\quad , \tag{66}$$

where S is again given by (65). Using the ω-values from Eq.(63) and an approximate value for alluminum alloy conductivity $\sigma \approx 3 \times 10^{17}\ \mathrm{sec}^{-1}$, we obtain from Eqs. (64)-(66)

$$Q(\mathrm{LOX}) \simeq 1.3 \times 10^4 \ , \qquad Q(\mathrm{LH_2}) \simeq 1.8 \times 10^4 \ . \tag{67}$$

If the energy U of a resonant mode is stored in a cavity, it decays at the rate

$$U = U_o \exp\left(-\frac{\omega t}{2\pi Q}\right) \tag{68}$$

where t is time and U_o is the energy at $t = 0$. If there is a power source P in the cavity, we will have

$$\frac{dU}{dt} = -\nu U + P \quad , \quad \nu = \frac{\omega}{2\pi Q} \ . \tag{69}$$

For constant P , a steady-state will be reached in a time (response time) of the order of ν^{-1}. From Eqs.(63) and (67) we get

$$T_{\mathrm{response}}(\mathrm{LOX}) \simeq \nu^{-1}(\mathrm{LOX}) = 1.1 \times 10^{-4} \text{ sec.}$$

$$T_{\mathrm{response}}(\mathrm{LH_2}) \simeq \nu^{-1}(\mathrm{LH_2}) = 4 \times 10^{-4} \text{ sec.} \tag{70}$$

From Eq.(69) we find the power necessary to maintain a given energy in the cavity

$$P = \nu U \ . \tag{71}$$

The energy U can be easily computed in terms of the electric field inside the cavity [9] ,

$$U(LOX) = \frac{L}{2} K^2 \int_0^{2\pi} d\phi \int_0^R r dr \, J_o^2(x_{01} r/R) \simeq 0.85 \, K^2$$

where the electric field is defined in Eq.(44), and U and K are given in joules and volts/meter respectively. The value of K is determined by the sensibility of the receiving antenna (see Sec. IV.5); an electric field intensity of 10^{-4} V/m. is well within the sensibility of present antenna technology.

For $r = 0.6\ R$, $J_o(x_{01}\ r/R) \simeq 1/2$ and we find

$$K(LOX) = 2 \times 10^{-4} \text{ V/m}$$

and

$$U(LOX) = 3.4 \times 10^{-8} \text{ joules.} \qquad (72)$$

Similarly, we obtain

$$U(LH_2) = 3 \times 10^{-6} \text{ joules} \ . \qquad (73)$$

From Eqs.(70)-(73) we get the power required for the measurements:

$$P(LOX) \simeq 0.3 \text{ mW} \ , \qquad (74)$$

$$P(LH_2) \simeq 7 \text{ mW} \ .$$

For the other two tanks not studied in detail in the last section, the power required would be of the order of the second quantity in (74). Thus, on the whole, a power of the order of 0.02 W will be required, intrinsecally, for the realization of the measurement.

IV. *FINAL CONSIDERATIONS*

The cavity resonator gaging system for measurement of propellant tank content under weightlessness conditions, is based on considering the tank as a resonant cavity, selecting an appropriate resonant mode whose frequency is determined on the ground under empty (or full) conditions, and detecting the new value of the frequency of that mode under the particular conditions of propellant content and configuration at a desired time.

The essential elements of this method would be a sweep oscillator, a coaxial line that connects it to an input probe in the tank, a receiving antenna, and a detector which by means of a signal conditioner would allow digital reading of tank content to be performed inside the spacecraft. A coaxial line appears appropriate for the resonant frequencies found in the previous section.

This gaging system satisfies well the general specifications indicated earlier in this report. Specifically, little modifications of the tank would be needed (just introduction of a receiving antenna and an input probe), weight and size of components are minimal, and the response time and power consumption of the method are optimal.

The measurement error of the method, calculated in this report for some Shuttle tanks, is reasonable, although for certain

propellant configurations exceeds somewhat the bounds suggested in Sec.II.1. It should be understood however that the calculations just mentioned were performed, for every tank considered, on the basis that the selected mode was the fundamental one. As observed in Sec.III, the measurement error would decrease if an (appropriate) higher mode were selected. The experimental detection of such modes is made easier by the fact that the Q - factor of the tanks is quite large ($Q \simeq 10^4$), and by the use of electric field sensors on the tank walls. These sensors would allow determination of mode characteristics. For the particular case of the Shuttle tanks, these characteristics, as shown in Sec.III, would be that the electric field of the mode were parallel, or perpendicular, to the main axis of the tank, or were independent of distance along, or from, that axis, or of azimuthal angle around it.

REFERENCES

1.- "Capacitance propellant gaging study for orbiting spacecraft" Transonics Inc. June 1967 NASA-CR-87496.

2.- "Feasibility Study for the development of a vaporizing-liquid-fuel gauge"
E.Fraga, A.Muñoz Torralbo - ESRO CR-19-July 1970.

3.- "Propellant Gauging Utilizing Radio Frequency Techniques"
G.A. Burns, Air Transport and Space Meeting, New York City, April 1964, Paper No. 870 B.

4.- "Zero-G Propellant Gaging Utilizing Radio Frequency Techniques in a Spherical Resonator".
R. Garriot and G.A. Burns IEE Transactions in Aerospace, Vol. AS-3, February 1965.

5.- "Positive Gaging System Feasibility Study",
NASA CR 102062, February 1968.

6.- "Interaction between cold plasmas and guided electromagnetic waves",
S. J. Buchsbaum, L. Mower and S.C. Brown, The Physics of Fluids 3 , 806 (1960).

7.- Technical Report No. 66, Research Laboratory of Electronics, M.I.T.,
S.C. Brown et al. (1948).

8.- "Methods of Mathematical Physics"
R. Courant and D. Hilbert. Interscience Publishers. N.York (1953).

9.- "Classical Electrodynamics",
J.D. Jackson, J. Wiley & Sons, Inc., New York, (1962).

10.- "Effect of contact angle and tank geometry on the configuration of liquid-vapor interface during weightlessness"
D.A. Petrash and all. NASA TN D-2075 (Oct.1963).

CRITICAL ACCELERATION FOR SURFACE TENSION GOVERNED PROPELLANT CONFIGURATIONS

Bond Number $B = \frac{\rho L^2 a^*}{\sigma} = 1$

ρ = Density

L = Characteristic lenght

a^* = Critical acceleration

σ = Specific surface tension

L cm.	$a^*_{LH_2}$ cm/sec^2	a^*_{LOX} cm/sec^2
1	32.5	9.14
10	0.325	9.14×10^{-2}
10^2	3.25×10^{-3}	9.14×10^{-4}
10^3	3.25×10^{-5}	9.14×10^{-6}
10^4	3.25×10^{-7}	9.14×10^{-8}

TABLE I

PHYSICAL PROPERTIES OF THE PROPELLANTS

		LO
BOILING TEMPERATURE AT ATMOSFERIC PRESSURE	$T^*(N.B.P)$	90,0
DENSITY AT ATMOSFERIC PRESSURE (LIQUID PHASE)	ρ^*	1,4
SURFACE TENSION (IN CONTACT WITH ITS VAPOR)	σ	13,2
RELATIVE DIELECTRIC CONSTANT	$\varepsilon/\varepsilon_0$	1,5

TABLE II

MAIN TANK

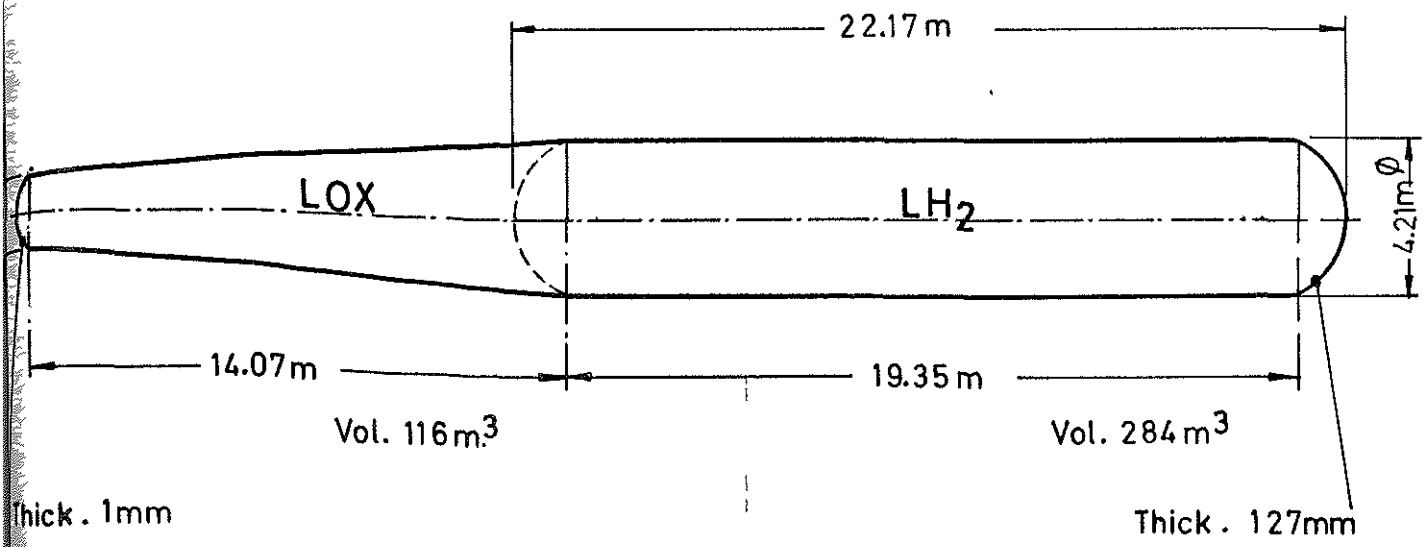

SECONDARY TANKS

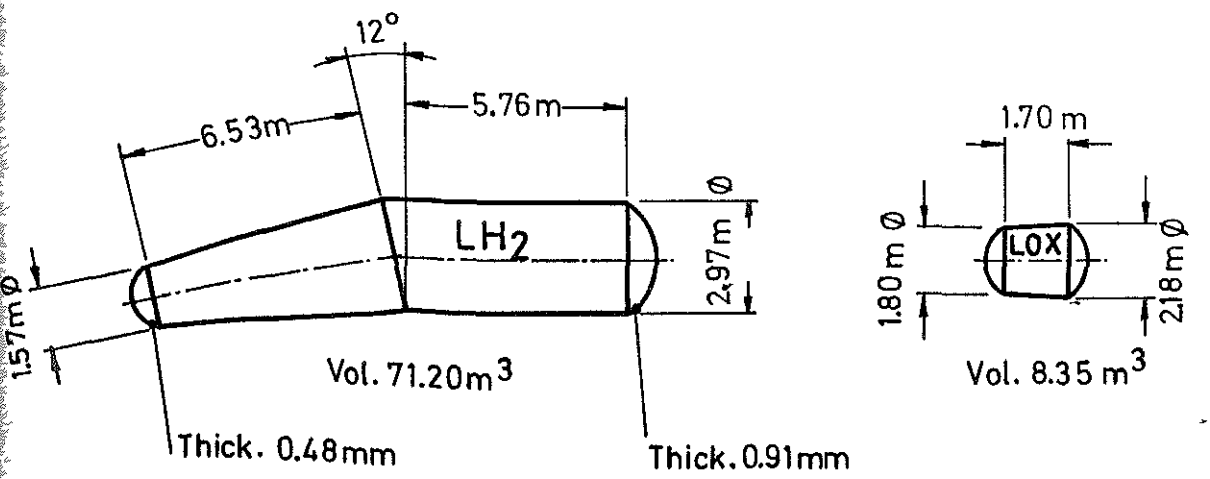

FIGURE I

FIG. Nº II

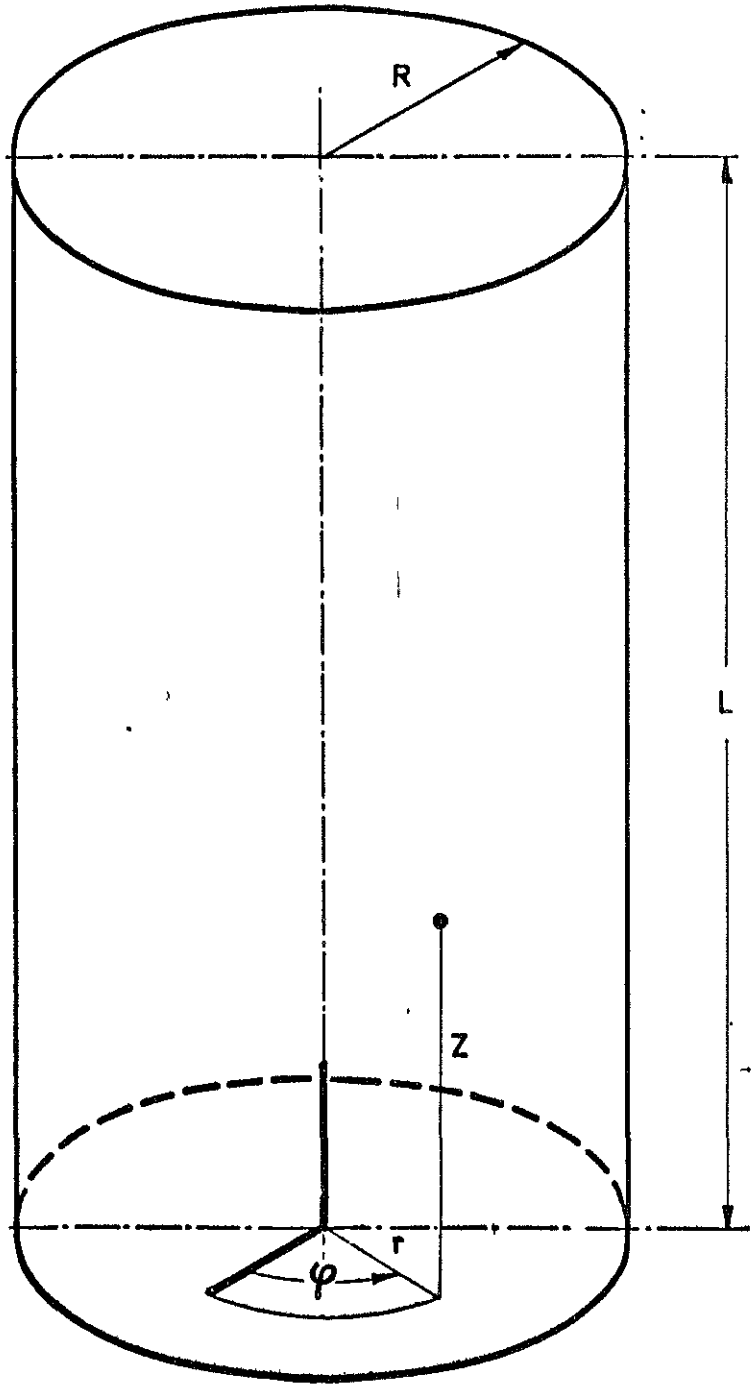

FIG. No III

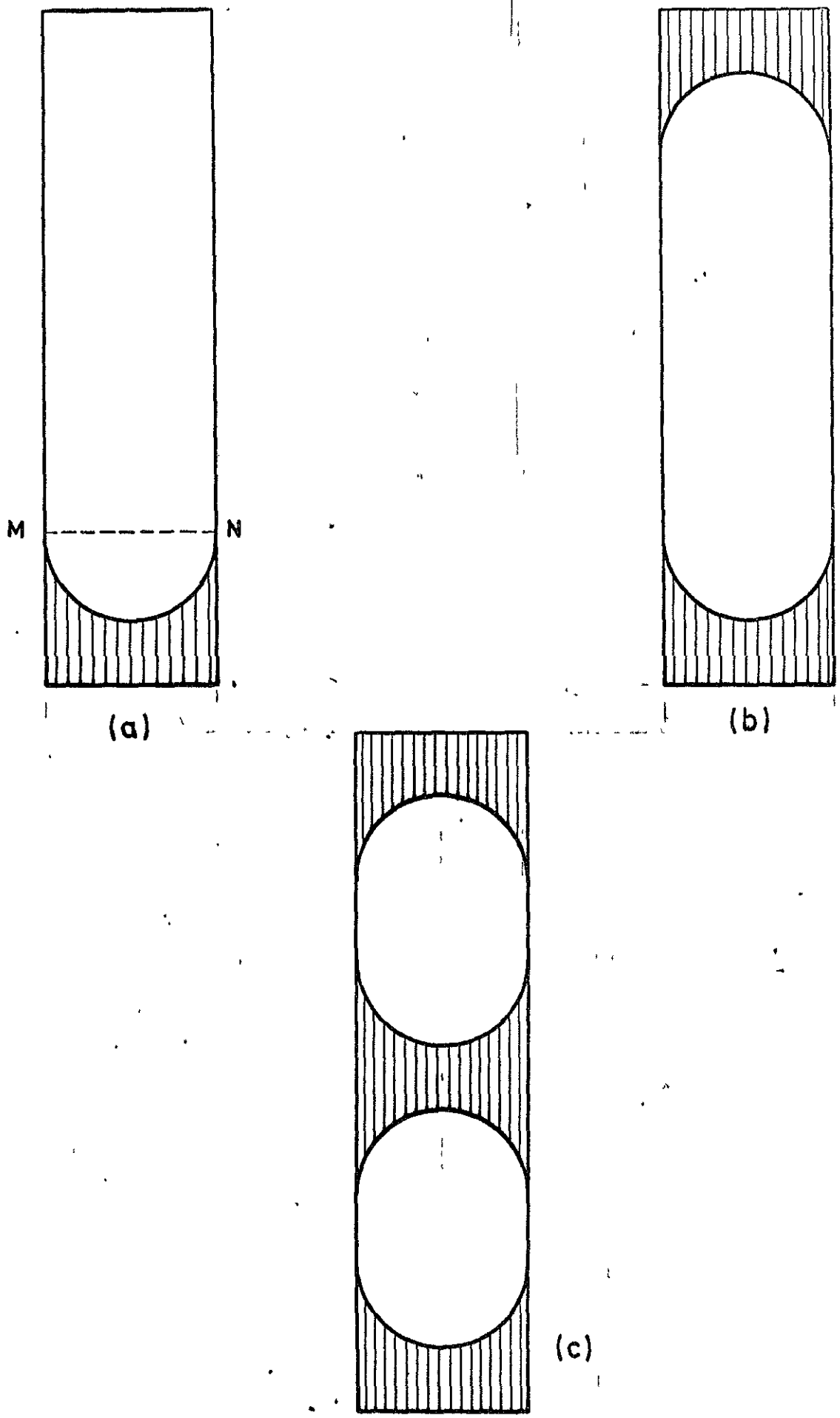

LIQUID CONFIGURATION WHEN SURFACE TENSION DOMINATES

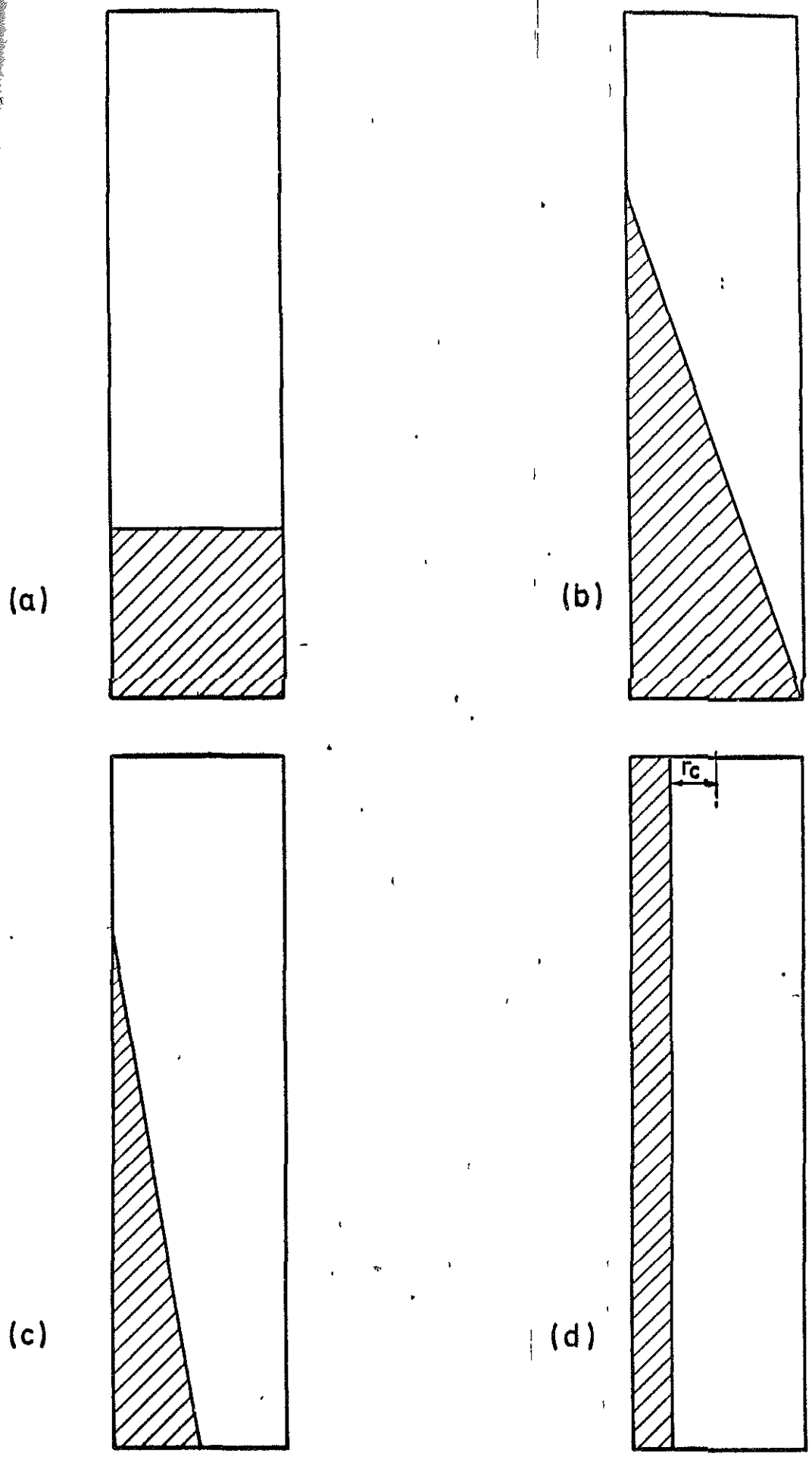

LIQUID CONFIGURATION WHEN ACCELERATIONS DOMINATES